Journal of Thermal Engineering
https://jten.yildiz.edu.tr/
https://doi.org/10.47481/jten.0094

RESEARCH ARTICLE

Cleaner combustion of bio-based rice bran oil diesel fuel using titanium oxide nanoparticle additives in single cylinder diesel engines

K. Sunil Kumar[1,*]

[1]Department of Mechanical Engineering, Saveetha School of Engineering, Saveetha Institute of Medical and Technical Sciences, Chennai, 602105, Tamil Nadu, India

Abstract

This experimental study focuses on rice bran blends with different proportions, followed by RB90D10 + 30 ppm TiO_2, RB80D20 + 30 ppm TiO_2, RB70D30 + 30 ppm TiO_2, RB50D50 + 30 ppm TiO_2, and Diesel. All the experiments are conducted in a single-cylinder diesel engine to measure performance, combustion, and emission characteristics. The engine brake thermal efficiency is good for the RB70D30 + 30 ppm TiO_2 blend, at 37%, which is greater than the diesel brake thermal efficiency, and the least specific fuel consumption is observed for the RB70D30 + 30 ppm TiO_2 blend, at 0.22 kg/kWh. The inline cylinder pressures are good for the blend RB50D50 + 30 ppm TiO_2, followed by 69 bar. The maximum HRR is attained for the blend RB50D50 + 30 ppm TiO_2, followed by 59 kJ/°CA. The blend RB80D20+30 ppm TiO_2 shows the lowest CO emissions, followed by 0.034% CO_2 and 0.034% NOx emissions; CO_2 and NOx emissions are lower for Diesel at 10.5% and 910 ppm, respectively. HC and Smoke opacity are lower for RB50D50+30 ppm TiO_2, followed by 22 ppm and 50 ppm, respectively. Thus, by promoting greener and bio-friendly fuels for vehicles and SDG 9 with the creation of cutting-edge nano fuel solutions for high-efficiency engine designs, our investigation directly contributes to achieving the Innovative nano fuel solutions for vehicles with high performance.

Keywords: TiO_2, rice bran biodiesel; combustion, performance, pollutants, fuel consumption, SDG goals

Cite this article as: Kumar, K. S. (2026). Cleaner combustion of bio-based rice bran oil diesel fuel using titanium oxide nanoparticle additives in single cylinder diesel engines. Journal of Thermal Engineering, 12(6), 2221–2232. https://doi.org/10.47481/jten.0094

1. Introduction

The depletion of fossil fuels is increasing worldwide. The depletion is due to the rapid use of Automobiles, and people across regions, from rural to urban areas, have a strong urge to use them [1]. The major drawbacks of using petrol- and diesel-based fuels include significant health issues, the continuous depletion of these fossil fuels, leading to their degradation and serious environmental impacts that affect respiratory issues and cardiovascular diseases, pollute the air, worsen climate change, and cause acid rain [2]. Harmful gases, such as nitrogen oxides, released into the atmosphere with a low water content, may cause serious harm to aquatic life. Another serious harm to aquatic life. Another serious issue people face regarding pollution is the release of CO_2, UHC, and CO from fossil fuels, which can cause serious health issues, especially for older people who are more susceptible to these gases, leading to eye disorders [3]. Hence, many researchers focus on alternative fuels, such as extracting oil from cottonseed, soybean seeds, and bitter gourd seeds. Although several studies have been conducted and experimentation has been carried out, researchers have demonstrated that the incorporation of biofuels [4].

Alternative fuels with light diesel proportions improve engine performance by 7% to 10%, while biodiesel-based fuels decrease Brake thermal efficiency by 8% to 33%. This is due to the oxygen content in biodiesel, which accelerates fuel evaporation and improves its atomization capacity compared to diesel [5]. Basically, biodiesel is a good fuel. It is an environmentally friendly fuel that offers enormous benefits, with very low emissions and greater density. The presence of oxygen at higher proportions 12% to 15% higher than in diesel improves engine performance, accelerates combustion, and decreases emissions compared to diesel. The researcher proved that increase in brake thermal efficiency by 7%, when the addiction

*Corresponding Author
E-mail Adress: sunilkumarkresearcher@gmail.com

Submitted: 28 March 2026; **Accepted:** 27 July 2026

This paper was recommended for publication in revised form by Editor-in-Chief Ahmet Selim Dalkılıç

of rice bran oil up to 20% and 80% diesel, but it is also observed that increase in NOx emissions for the proportion of 30% rice bran oil and 70% diesel, the reduced emission is observed for the fuel 100% rice bran oil, because the shortest ignition delay is observed for the fuel compared with diesel and other blends [6]. The researcher then demonstrated that 10% soybean oil in 90% diesel (B10) improved BTE by 4.6% and reduced BSFC by 8.33% compared to diesel. The HRR for the same blend is 60 kJ/°CA to achieve the lowest emissions. CO_2 is lowest for the pure soybean blend, with a reduction of 8.32% compared to diesel; HC is very low at 9.7% compared to diesel; and NOx is lower at 7.2% compared to diesel. An increase in engine vibration is observed for the blend containing 30% pyrolysis oil and 70% diesel [7]. Compared to diesel and pyrolysis blends. A lower cetane number affects engine performance.

The increase in the percentage of pyrolysis oil affects engine performance at a lower rate than diesel. The researcher [8] tried the addition of various nanoparticles to the biodiesel blends has enormous benefits in terms of reduced emission particulates Hence the researchers tried XRD, SEM and TGA additives of the nano particles concerned to TiO_2, CeO_2 with various proportions followed by 5 ppm, 10 ppm, 15 ppm, 20 ppm, 25 ppm has potential advantages in terms of increase of calorific value, reduced brake specific fuel consumption, increased HRR, increased cylinder pressures, reduced HC, NOx, CO, CO_2 emissions from diesel. The utilisation of canola seed oil biodiesel significantly diminished particles and emissions of carbon monoxide CO with an increase in brake mean effective pressure. Emitted nitrogen oxides rose slightly owing to the inherent presence of nitrogen oxides in biofuel [9]. The diesel engine operates on a mixture of canola oil and diesel, augmented by aluminium oxide particles. The Taguchi method's signal-to-noise ratio approach, grey predictive approach, and response spectrum approach are utilised to optimise brake thermal efficiency, while minimising nitrogen dioxide emissions and fuel costs. The criteria examined to influence are the proportion of canola oil in the blend, the number of nanoparticles, the ignition velocity, and the energy injection timing [10]. The anticipated best possible outcomes are evaluated for accuracy and demonstrate a reasonable concordance. The optimal configuration is determined to be a total of 18% canola oil mixture, with a small particle dosage of 30 parts per million, an energy injection of 210 bars, and a combustion injection period of 21° before top dead canter (bTDC). This mixture enhances brake thermal efficiency by 16% and decreases nitrogen oxides in the exhaust by three percentage points compared to diesel fuel [11]. This study examined the engine performance of five distinct biodiesels derived from five plant-based oils maize, sunflower, soybean, canola seed, and hazelnut against one another and against diesel fuel within an identical research framework. Biofuel experiments were conducted with 20% and 50% biodiesel in diesel fuel, following biodiesel production via transesterification. Each was used as fuel in the diesel-powered engine. Both successful and suggested parameters were assessed for each fuel following performance testing. The mixture containing 20% pistachio biofuels demonstrated the highest efficiency [12].

This research addresses the issue of utilising canola oil and n-hexane blends in diesel-powered vehicles equipped with common-rail fuel injection systems. It enhances the preparation mechanism of the explosive cocktail and affects the combustibility activity [13]. According to [14], the performance and emission attributes of a dual-cylinder, moringa oleforia biodiesel blend with aluminium oxide as a catalyst were identified as the best results in terms of efficiency and the least emissions. The results demonstrated that chemically treated mixtures reduced emissions and NOx levels and increased brake thermal efficiency compared with unprocessed diesel fuel [15]. The results indicate that small quantities of canola oil (with fungicides) could be a growing, environmentally sustainable alternative to conventional diesel fuel, particularly in areas where wheat is grown. According to [16], sunflower oil with diethyl ether improves the bulk density and surface tension of the studied blends, which were dramatically reduced when DEE was combined with SO. Consequently, DEE enhances the dispersion of the SO introduced into the combustion chambers.

Building on earlier research, this work incorporates several novel improvements to understand better how TiO_2 nanomaterials affect the performance and pollutant attributes of diesel cars powered by rice bran biofuels. A comprehensive assessment of combustion behaviour and emissions from biofuel mixtures derived from TiO_2 Nano-Refined Rice Bran under various engine operating conditions provided a better understanding of fuel behaviour throughout the entire operating period. This work provides a complete description of flame properties that were not necessarily presented simultaneously in previous work. The combustion properties studied include in-cylinder pressure, thermal discharge rate, ignition delay, and combustion kinetics, which are not always reported together in previous studies. The novelty of this study is not just the use of TiO_2 nanoparticles in producing rice bran biodiesel but also the comprehensive evaluation of fuel durability, combustion kinetic parameters, engine function and emission profile, along with the mechanistic explanation of the perceived improvements, which provides a complete understanding of the combustibility improvement in rice bran biodiesel in the context of its use in diesel-powered automobiles.

The literature and exploratory assessments were used to choose the 30 ppm TiO_2 particles. The effect of various particle strengths on engine performance, fuel balance, dispersion coherence and pollutant parameters has been evaluated. Ultimate burning output was only slightly influenced by concentrations < 30 ppm, whereas energy homogeneity was negatively impacted by increased particle grouping. The amount of pure oxygen was found to be optimal when the level was limited to 30 ppm, in terms of catalyst effectiveness, fuel endurance and motor performance. The amount of TiO_2 nanoparticles enhanced the fuel atomization and burning performance but did not significantly alter fuel properties or lead to deposition. Compared with the conventional fuel, the decreased emissions of moisture, oxygen, smoke visibility and the increase in brake thermal efficiency were largely due to improved combustion characteristics. Moreover, previous studies on TiO_2 nano-additive in diesel–biodiesel blends reported that doses ranging from 20 ppm to 50 ppm could be useful for improving combustion and emission properties.

2. Materials and methods

2.1. Materials

All the materials were purchased from the local dealer in chennai, as mentioned in Table 1. The diesel is purchased from the local dealer in Kancheepuram at Rs 100 per litre. The pure rice bran oil is purchased from a different dealer in Hyderabad for Rs. 700 per litre. TiO_2 was purchased in Chennai at Rs 600 per kg. All the materials used in this process were purchased for this project at reasonable costs. Table 1 illustrates the materials used in this analysis.

Table 1. Materials

S. No	Materials	Cost	Quantity	Supplier
1	Diesel	200	2 litre	Kancheepuram
2	Rice bran Oil	700	1 Litre	Hyderabad
3	Titanium Oxide	600	1 kg	Chennai

2.2. Methods

2.2.1. Blends preparation

Under controlled conditions, the unrefined rice bran grease was trans esterified to produce biofuels using alkaline catalysts such as methanol and 5% KOH. The grain-based oils were boiled to remove water, and the precipitate was filtered off. The reaction was then performed at a set temperature for a set period, with regular stirring to ensure the reaction was complete and all esters had been converted. The products of the reaction were filtered through a funnel, and the glycerol portion was separated from the biofuel layer because of the difference in density. The biodiesel produced was washed with lukewarm purified water to remove detergents, unincorporated alcohols and catalytic residues. The cleaned biodiesel was then gently boiled and stored in tightly closed bags to obtain a sufficient amount of rice bran methyl ester for further use.

2.2.2. Test fuel preparation

The controlled study fuels were prepared with rice bran biodiesel and mineral diesel in various ratios. The mixes investigated in the present study were RB90D10, RB80D20, RB70D30 and RB50D50, where each diesel-biodiesel blend was supplemented with 30 ppm of metallic oxide nanostructures, titanium dioxide, to assess the effect of low levels of metallic oxide on diesel-biodiesel combustibility enhancement. Clean diesel is used as fuel. The required amount of TiO_2 particulates was determined using a precision device and then added to each combustion mixture. The mixes were mechanically stirred initially and then ultrasonically agitated for a certain time to ensure suspension stability and eliminate particle aggregation. This step helped to disperse the microscopic particles throughout the fuel system before the fuel was sent to the ignition system. For uniformity and to minimise precipitation, fresh mixes were developed prior to testing. The standard rice bran biodiesel was blended with diesel fuel, and various amounts of surfactant were added to improve the dispersion stability of the blend, as demonstrated by TiO_2 particles.

2.3. Methodology procedure

2.3.1. Biodiesel preparation procedure

The traditional transesterification method was used to produce rice bran oil biodiesel. The conventional rice bran oil-alcohol reaction process was conducted with a neutral catalyst and under controlled heating and agitation. Once the reaction was finished, the biodiesel and triglyceride phases were separated, and the biodiesel was continually washed and dried to obtain biodiesel that conforms to typical biodiesel composition standards.

Biodiesel was prepared from rice bran oil using the traditional method of alkali-catalysed transesterification process. The extracted rice bran oil was then filtered to remove impurities, heated at 104°C for approximately 30 minutes to remove moisture, and then cooled to the reaction temperature. The alcohol used was 80% chemical methanol, while the catalytic agent was in fact sodium hydroxide (NaOH). A solution of 1% Hydroxide (by oil volume) in alcohol containing 6 molecules of methamphetamine to one molecule of alcohol was prepared. The methoxide-based fluid was subsequently slowly added to the heated rice bran oil, which was stirred at 600 rpm. The transesterification reaction time was 90 minutes at 60 ± 2 °C in the presence of air. After completion of the kinetic reaction, the aggregate was moved to a dividing funnel and left to stratify under a vacuum for 12 hours to separate the biofuel and glycerin fractions. The lower layer with glycerin was removed, and the upper layer with biofuel was rinsed 3-4 times using academic distilled water at a temperature of 50-60 °C. The rinse water should be neutral in pH.

2.3.2. Dispersing the nanoparticles

Regular titanium dioxide (TiO_2) particles were added to the rice bran biofuels at a concentration of 30 parts per million (ppm). The nanoparticles were first introduced and then processed using ultrasonic vibrations and traditional magnetic mixing to ensure even dispersion of the particulates in the fuel-based blend and prevent clumping. The conventional TiO_2 nanoparticles of the typical size of 20-30 nm and 99 per cent purity were used. The correct amount of TiO_2 nanoparticles (± 0.1 mg) was determined using a precision balance and then gradually added to the biofuel blend. The liquid was first blended with a magnetic stirring apparatus for 30 min at 800 rpm for preparatory blending. Next, the liquid fuel mixture was ultrasonicated in an ultrasonic bath for 45 min at 200W and 40kHz to disrupt particle aggregation and form an intact, non-aggregated homogeneous suspension. The low concentration of nanoparticles did not cause distribution problems during the experiment; thus, no surfactant was used. In different engine-based tests, the mixture was carefully stirred to obtain a uniform dispersion of the nanoparticles. The manufactured nano fuel was kept in opaque amber sample bottles to avoid particle settling within 24-48 hrs under normal lab conditions. Table 2 summarises the reactions involved.

Table 2. Summary of the reactions

S No	Parameter	Value
1	Catalyst concentration	1 wt.% of oil
2	Feedstock	Rice bran oil
3	Magnetic stirring	800 rpm, 30 min
4	Alcohol	Methanol
5	Particle size	20–30 nm
6	Nanoparticle concentration	30 ppm
7	Nanoparticle	TiO_2
8	Drying time	1 h
9	Storage	Airtight amber bottles
10	Drying temperature	105°C
11	Ultrasonication	40 kHz, 200 W, 45 min
12	Washing medium	Warm distilled water (50–60°C)
13	Settling time	12 h
14	Reaction time	90 min
15	Stirring speed	600 rpm
16	Reaction temperature	60 ± 2°C
17	Methanol-to-oil molar ratio	06:01
18	Catalyst	Sodium hydroxide (NaOH)

2.3.3. Stability of the nanoparticle–fuel blends

Deposition of TiO_2 fuel nanoparticles over a certain storage time was visually measured to evaluate the above-mentioned systems' sustainability. Good dispersion consistency was indicated, as no phase separation or particle settlement was observed. A consistent particulate suspension was ensured by magnetisation and ultrasonics during the investigation. TiO_2 nanoparticle-fuel mixes were evaluated using a settling test for their stability. These were then exposed to an additional 30 minutes of magnetisation in opaque, closed glass bottles and then 45 minutes of ultrasonics under ambient air conditions in the laboratory. The mixtures were visually inspected at regular intervals for 30 days for any appearance of phase dissociation, sludge or aggregation of nanoparticles. No phase differentiation occurred during the period of record, or only particulate sedimentation occurred, indicating a high degree of dispersal consistency during the period of record. The particulate distribution was uniform, and fuel characteristics were uniform for each combustion test through complete mixing of thorium for 2-3 minutes before the combustion test. The properties of blends are given in Table 3.

Table 3. Properties of blends

Property	ASTM D6751	Diesel	RB90D10+ 30 ppm TiO_2	RB80D20 + 30 ppm TiO_2	RB70D30 + 30 ppm TiO_2	RB50D50 + 30 ppm TiO_2
Fire point (°C)	165	159	161	164	169	164
Kinematic viscosity (mm^2/S)	1.9–6.0	4.3	4.4	4.7	5.2	1.9–6.0
Flash Point (°C)	95	140	145	150	155	95
Density @15°C	860-900	873	877	881	892	860–900
Cetane number	48	51	53	55	59	48
HHV MJ/Kg	42.1-45.1	41.9	41.6	41.3	40.6	39.9
Air/fuel ratio	10-14	14.87	12.1	13.1	12.4	13.7

The TiO_2 particles were added to the blends. The increase in fire resistance from 161 °C for blend RB90D10 to 169 °C RB70D30 provided added safety in handling and storing scholarly materials due to the added biofuel content. The increase of 4.4 to 5.2 mm^2/s in elastic viscosity reflects the inherently higher fluidity of biofuels compared to conventional diesel. Further enhanced fuel protection was validated, as the rapid threshold was raised from 145 °C to 155 °C. The density of the biodiesel also slowly rose from 877 kg/m^3 to 892 kg/m^3, and the Cetane number increased from 53 to 59, which would be beneficial for reducing the ignition delay and improving combustion efficiency. It was observed that the HHV reduced from 41.6 to 40.6 MJ/kg, which shows that the energy density of biodiesel is less than that of the conventional fuel.

3. Experimental procedure

The apparatus comprises an automobile engine with one cylinder and four strokes, linked to a preload measurement device of the swirling current type. It comes with all the tools needed to assess crank angle and ignition temperature. Figure 1 illustrates the experimental setup used in this study. The combustion indication for the Pθ−PV schematics interfaces the signals with the computing system. Communication with fuel circulation, air movement, humidity, and loading measurements is also accommodated. The setup comprises an independent circuit box containing the following components: a breathing box, a fuel reservoir, a speedometer, a fuel monitoring device, emitters to monitor the quantities of both air and fuel, and processing and combustion indicators [17]. The engine was allowed 15 to 20 minutes of operation to reach steady-state operating conditions for each test before use. Equilibrium was verified by monitoring key parameters, including engine speed, exhaust temperature, fuel consumption, and water outlet temperature. Table 4 represents engine specifications.

Figure 1. Experimental setup

Table 4. Engine Specifications

SNO	Description	Specifications, Type and Capacity
1	Engine	4 stroke Engine
2	Dynamometer	Eddy current, water cooled
3	Power	5.2 kW
4	Speed	1500 rpm
5	Overall dimensions	W 2000 x D 2500 x H 1500 mm
6	Propeller shaft	Universal joints
7	Stroke	116 mm
8	Bore	90 mm
9	Air box	Mild steel fabricated
10	Fuel tank	Capacity 15 litres
11	Calorimeter	Pipe type
12	Crank angle sensor	Resolution 1 Deg, Speed 5500 RPM with TDC pulse
13	Data acquisition device	NI USB-6210, 16-bit, 250kS/s.
14	Piezo powering unit	Model AX-409.
15	Temperature sensor	Type RTD, PT100 and Thermocouple, Type K
16	Temperature transmitter	RTD Type
17	Swept volume	666 cc
18	Compression ratio	18 :1
19	Injection Pressure	220 bar
20	Injection timing	23° bTDC

4. Uncertainity analysis

To ensure the accuracy and repeatability of experiments, Kline and McClintock's diffusion-of-errors approach was used to perform the uncertainty analysis. All instruments were calibrated as required before experimentation, and each experiment was performed three times under similar operating conditions. For the examination, mean values were used, and ambiguities in the parameters analysed were determined based on the method's reliability. The evaluation of uncertainties in a combustion cylinder involves detecting, characterising, and assessing ambiguities related to evaluations, model estimations, and performance characteristics throughout the engine's operation, assessment, or simulation. Uncertainty investigation in a diesel engine involves a comprehensive evaluation of potential errors or variations in operating parameters, including engine power, performance, emissions, and energy expenditure, arising from imperfections in testing equipment, laboratory configurations, surroundings, and assumptions. Table 5 defines the accuracy of measuring instruments. The % uncertainty for each observed parameter was computed as in Equation (1) [18].

$$\Delta E = \frac{2n_i}{n_i} * 100 \quad (1)$$

ΔE = Net accuracy using Gausian relational factors

n_i = Readings calibrated in maximal counts.

Equation (2) referred to in [19] represents the overall inaccuracy of all the instruments used in the studies. Each instrument has a finite measurement error associated with it, caused by its calibration at a specific sensitivity, the accuracy of its sensor, ambient conditions, and operating limitations. These individual errors are added together to calculate the total calibrated inaccuracy (R), which is used to evaluate the reliability and accuracy of the experimental results.

$$R = f(E1, E2, E3 \ldots \ldots \ \ldots \ldots \ \ldots En) \quad (2)$$

R = Net calibrated error

E1,E2,E3 = Errors occured during different calibrated set of readings

The third equation explicitly delineates the real variances and associated judgments of the tiny mistakes encountered throughout the experiments, including the precise quantity of facts, potential cycles, and the associated uncertainty.The conventional uncertainty propagation formula using the root-sum-square (RSS) technique is shown as Equation (3), referred to from [20]. It measures the overall uncertainty of a statistic calculated from a set of values that are quantifiable and independent of each other. Each metric has an influence determined by its sensitivity metric, which indicates how sensitive it is to changes in itself. Since the error measurements are unbiased and randomly scattered, the total ambiguity is obtained by taking the square root of the sum of the squares of the individual error measurements. This method can be used to obtain a valid estimation of the overall experimental uncertainty and is widely used in academic physics and heat transmission studies.

$$\Delta R = \sqrt{\left(\frac{\partial R}{\partial E_1}\Delta E_1\right)^2 + \left(\frac{\partial R}{\partial E_2}\Delta E_2\right)^2 + \left(\frac{\partial R}{\partial E_3}\Delta E_3\right)^2 + \ldots\left(\frac{\partial R}{\partial E_n}\Delta E_n\right)^2} \quad (3)$$

The tests were performed on three separate occasions under the same conditions for all fuel blends and operational states to ensure the repeatability and reliability of the measured results. The efficiency, burning, and pollutant data are averages of three observations. Repeatability of the experimental process was established. Table 6 represents the measure of Uncertainty.

Table 5. Accuracy of measuring instruments

S. No	Parameter	Instrument Accuracy
1	NO_x emission	± 12 ppm
2	CO emission	±0.02 % vol
3	HC emission	±8 ppm
4	Exhaust gas temperature	± 2 °C
5	Engine speed	± 5 rpm
6	Load measurement	±0.4 kg
7	Fuel consumption	±0.2 mL
8	Smoke opacity	±2.1 %

Table 6. Measure of uncertainity

S.No	Parameter	Uncertainty (%)
1	NO_x emission	± 1.6
2	Smoke Opacity	± 1.2
3	HC Emission	± 1.8
4	Exhaust Gas Temperature	± 0.5
5	Brake Thermal Efficiency	± 2.1
6	Brake Specific Fuel Consumption	± 1.9
7	CO Emission	± 2.2
8	CO2 Emission	± 1.8

5. Results and discussion

5.1. Measurement of brake thermal efficiency

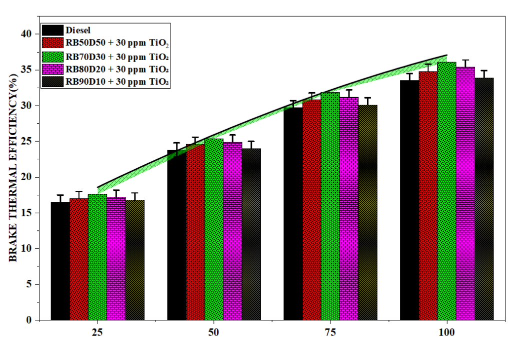

Figure 2. Brake thermal efficiency

The variation of brake thermal efficiency of the fuel-diesel blends rice bran fuel and diesel fuel with engine capacity when treated with TiO_2 nanomaterials is depicted in Figure 2. The increase in BTE is found to increase regularly as the horsepower increases for all oils investigated. In the transition region , where a larger fraction of the combustibility is utilised effectively into useful mechanical work, this tendency is accounted for primarily by the improvement in combustibility and by the decrease in heat transfer. Under all loads, the fuels which exhibit the highest thermal efficiency for brakes are Diesel, RB50D50 + 30 ppm TiO_2, RB80D20 + 30 ppm TiO_2, RB90D10 + 30 ppm TiO_2, and RB70D30 + 30 ppm TiO_2.

The blend of RB70D30 and 30 ppm TiO_2 has an aggregate BTE concentration of 37% at full load, which is higher than a 34% concentration for diesel. Blend RB70D30 + 30 ppm TiO_2 has an 8.8% higher BTE than diesel.This increase in efficacy is due to the oxygen-rich nature of biofuels and the catalytic characteristics of TiO_2 particles, which together encourage improved dissolution, higher air-fuel blending efficiency, and quicker oxidative responses during breakdown. An atmosphere containing TiO_2 nanoparticles is crucial for improving combustion effectiveness. They are so small and have such biochemical properties that they help further break down fuel particles and release more active oxygen molecules during ignition. Consequently, thermal efficiency increases because ignition occurs sooner and heating is more thorough [21].

5.2 Brake specific fuel consumption

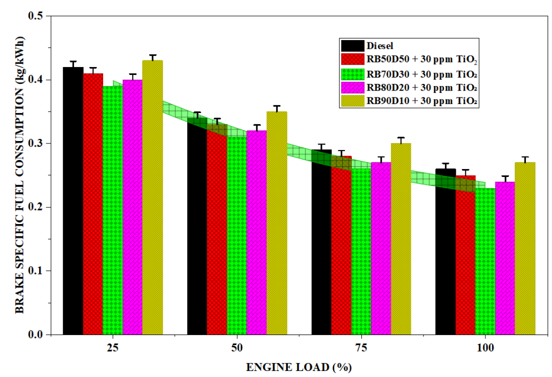

Figure 3. Brake specific fuel consumption

The brake-specific fuel consumption for various blends of rice bran and diesel fuel with 30 ppm of TiO_2 nanoparticles is compared with engine capacity in Figure 3. It's clear that for each fuel tested, BSFC decreases slowly with increasing engine usage. This is mainly attributed to the higher combustion rate and lower proportional heat transfer at higher loads, where a larger percentage of the total fossil fuel power generated is effectively converted to the desired productive activity. The two fuel reductions of 25% in loading result in higher BSFC values in all aspects because of the lack of combustion and lower ambient temperatures in the cylinder. With an increase in vehicle power from 25% to 100%, the internal pressure and temperature of the vehicle increase greatly, which enhances the three ways of dissipation: vaporisation and oxidation. This means that less fuel is consumed per unit of braking force provided. RB70D30 + 30 ppm TiO_2 has the lowest BSFC at all loading conditions when compared to clean diesel and other blends. The BSFC at full throttle for the RB70D30 + 30 ppm TiO_2 combination is approximately 0.22 kg/kWh, which is lower than the diesel product's 0.25 kg/kWh. The RB70D30 + 30 ppm TiO_2 combination has the lowest BSFC, 12% lower than diesel. This boost is due to the combination of oxygenation/biofuel and the catalytic effect of TiO_2 fragments that accelerate combustion, enhance air-fuel combustion, and deepen fuel oxidation. On the other hand, the fuel performance with respect to BSFC is relatively high for the RB90D10 + 30 ppm TiO_2 mixture among the fuels studied. The greater fluidity and reduced calorific value of biofuel blends are the main causes of this effect, which could result in worse vaporisation and somewhat more fuel use to achieve the same amount of power [22].

5. Combustion

5. 1. Cylinder pressures

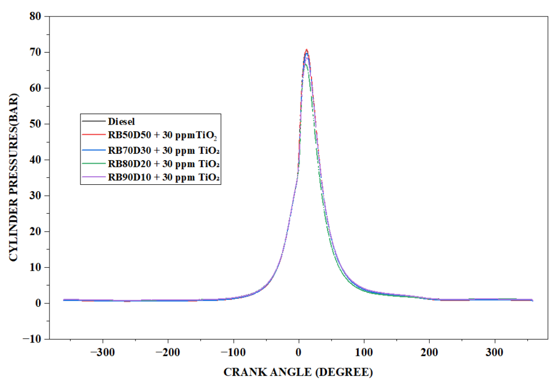

Figure 4. Cylinder pressures

For diesel and rice bran biodiesel blends doped with 30 ppm of TiO_2 nanoparticles. The variation of internal pressures with the crank position is shown in Figure 4. Among the blends evaluated, the blend RB50D50 + 30 ppm TiO_2 has the highest maximum chamber pressure of approximately 69 bar. However, diesel is capable of 65 bar. The combination of RB50D50 and 30 ppm TiO_2 yields a higher value of 6.2 % than diesel. Nanoparticulate materials are used to increase the rate of fuel–air interaction, improve mixing, and increase the rate of oxidation in a burning vessel. In addition, the oxygen in the oil will allow for more complete combustion, which would raise the temperature and air pressure of the chamber. The strength of the chamber steadily decreases during the enlarging strokes after the high-intensity due to increasing burning gases and to the approach of the crankshaft to the bottom dead centre [23].

5.2. Heat release rates

Figure 5 shows the difference in HRR against crankshaft angle for the various fuel mixtures used diesel fuel and rice bran diesel biodiesel with 30 ppm TiO_2 nanocrystals added. The HRR pattern can shed light on the power-releasing behaviour and the combustion parameters during the combustion rotation inside the combustion chamber. The blend of RB50D50 + 30 ppm TiO_2 exhibited the highest peak HRR value among the blends evaluated, followed by the biodiesel and RB70D30 + 30 ppm TiO_2 blends, while the peak HRR values for the RB80D20 + 30 ppm TiO_2 and RB90D10 + 30 ppm TiO_2 blends were relatively low. The heat release rate of the diesel is 55 kJ/°CA. The RB50D50 + 30 ppm TiO_2 gives a 7.2% improvement in performance compared to diesel.

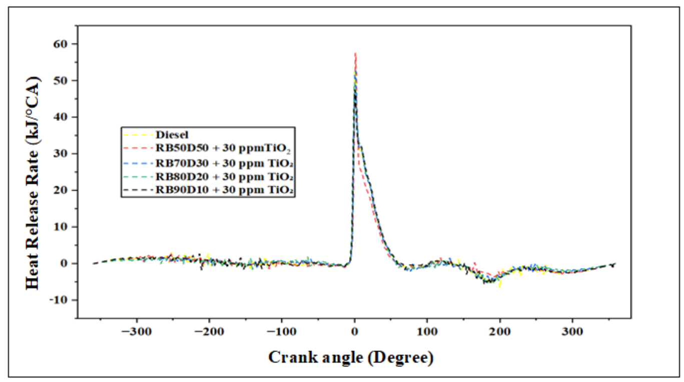

Figure 5. Heat release rates

At the end of the expansion stage of the RB50D50 mixture, the presence of TiO_2 nanoparticles and the saturating effect of biodiesel, which improves combustion properties, caused the HRR to be higher. In all the combinations, however, the HRR cross-sections level off at the end of the process, suggesting that most thermal degradation occurs after combustion. Furthermore, the consistency of HRR characteristics for all the fuels suggests that incorporating TiO_2 particulates and biofuel blends could help enhance fuel ignition without significantly changing the fuel-burning process . The catalytic oxidation system causes all of these: the typical oxygen-neutralising property and the improved heat conduction properties of the TiO_2 nanoparticles. These properties help achieve fuel atomisation, increase the rate of oxidation reactions, decrease ignition delay, and achieve complete combustion. This has a positive effect, such as fuel savings and improved brake thermal efficiency [24].

6. Emissions

6.1. Carbon monoxide

The reduction in carbon monoxide emissions with increasing power from diesel-rice bran biodiesel blends with 30 ppm TiO_2 particles is shown in Figure 6. CO emissions from all the fuels tested decrease as engine load increases. There are no significant differences in CO emissions between clean diesel and RB90D10 + TiO_2, but RB80D20

+ 30 ppm TiO_2 has a lower carbon footprint than RB70D30 + 30 ppm TiO_2 and RB50D50 + 30 ppm TiO_2 under any loading condition. The RB80D20 + 30 ppm TiO_2 blend produces 0.034% CO at full-throttle conditions, and diesel fuel produces 0.05%. The RB80D20+ 30 ppm TiO_2 blend has the lowest emissions, which are 32 % lower than the emissions from diesel. Oxygen molecules present in the chemical structure of biodiesel naturally improve the intermediate compound formation, which results in better combustion [25].

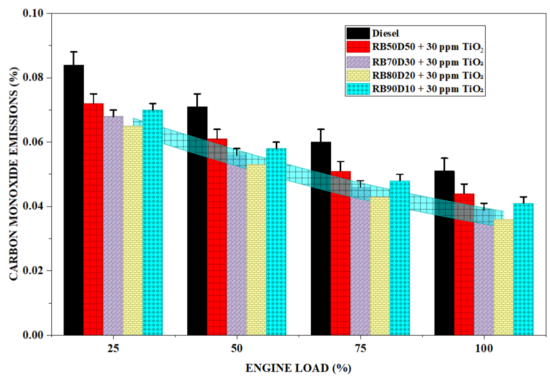

Figure 6. CO emissions

6.2. CO_2 Emissions

Figure 7 illustrates the trend of the CO_2 emission rate of the diesel and rice bran fuel-diesel mixtures containing 30 ppm of TiO_2 particles as a function of engine load. The more energy injected, the more CO_2 is released, due to increased internal heating within the engine. The fuels that have the highest CO_2 emissions under all loading conditions are RB50D50 + 30 ppm TiO_2, followed by diesel, RB70D30 + 30 ppm TiO_2, RB80D20 + 30 ppm TiO_2, and RB90D10 + 30 ppm TiO_2. At peak load, the RB50D50 + 30 ppm TiO_2 mixture produces approximately 12.6% CO_2, whereas the diesel mixture produces 10.5% CO_2. The composition of fuels produced from biodiesel fuel is oxygenated, which allows for better combustion [26]. Diesel emits the lowest number of emissions, followed by RB50D50 + 30 ppm TiO_2 blends at 16.6% CO_2.

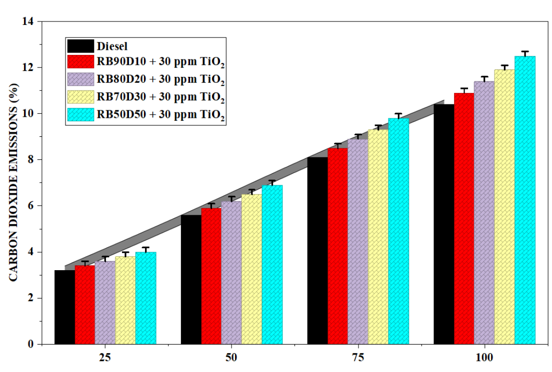

Figure 7. Carbon dioxide emissions

6.3. HC emissions

Diesel and diesel-rice bran biodiesel blends containing 30 ppm TiO_2 nanoparticles show how heterocyclic hydrocarbon pollutants change with engine workload in Figure 8. When fuel atoms depart the furnace unaltered or are imperfectly consumed, this is known as hydrocarbon emission. It is clear from Figure 8 that for all investigated fuels, greenhouse gas emissions diminish as engine workload increases. Due to oxidation of the air-fuel mixture and higher HC emissions, the flame temperature in the piston is rather low at lighter loads. The fuel with the lowest hydrocarbon emissions was RB50D50 + 30 ppm TiO_2, at 22 ppm. But diesel emits 42 ppm. The RB50D50 + 30 ppm TiO_2 blend is 47% lower than diesel. Because rice bran biofuels are oxygen-enriched, they facilitate more complete combustion, which is the main reason biodiesel blends reduce hydrocarbon emissions.

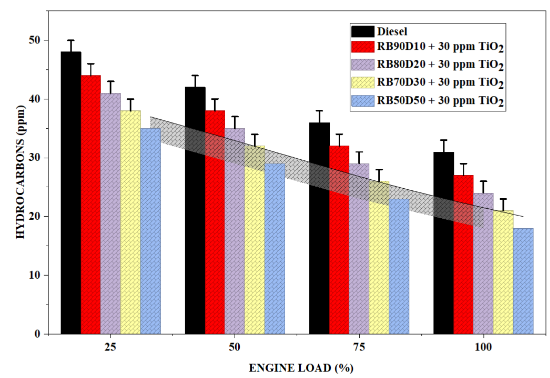

Figure 8. HC emissions

Biodiesel particles contain more oxygen than conventional fuel, and the amount of incompletely burned pollutants is reduced as a result of this oxidation process. TiO_2 atom fragments enhance the ignition characteristics as reactive regulators. This increased oxidation results in reduced content of compounds which are not fully oxidised in engine exhausts [27]. The blends of rice bran and TiO_2 generally had remarkable effects on the environment: the blends led to a significant reduction in hydrocarbon emissions compared with conventional diesel operation, particularly at higher cylinder loads.

6.4. NO_x Emissions

Figure 9 represents NOx emissions attained in this analysis. The inner-cylinder burning temperatures, the availability of air, and the duration of elevated pollutant levels are the three main factors that significantly impact NO_x pollution. It is clear from Figure 9 that NO_x emissions for all investigated fuels increase significantly with increasing engine power. This activity occurs when combustible oxidation events are amplified and engine-cylinder heating increases in response to increased fuel induction, both of which are driven by increased workloads [28]. The Zeldovich procedure, in which oxygen and nitrogen combine at elevated levels to produce oxides of nitrogen, is enhanced by the rise in ignition temperature, which in turn increases the generation of thermally generated NO_x. Overall, the NO_x pollutants from biodiesel-diesel mixes containing TiO_2 nanocrystals exceed those from normal diesel oil.

In contrast to the nanoparticle-driven combinations, diesel yields around 910 ppm at its full capacity. RB90D10 + 30 ppm TiO_2 achieves NOx emissions of 980 ppm. This is 7.14% greater than diesel. Due to its higher oxygen content, rice bran biofuel will increase the oxidation rate in air-fuelled combustion, raising the maximum burning temperature and leading to higher NO_x emissions in biofuel blends. In addition, the combustibility catalysts, which work through TiO_2 nano-materials, promote combustion and ignition [34].

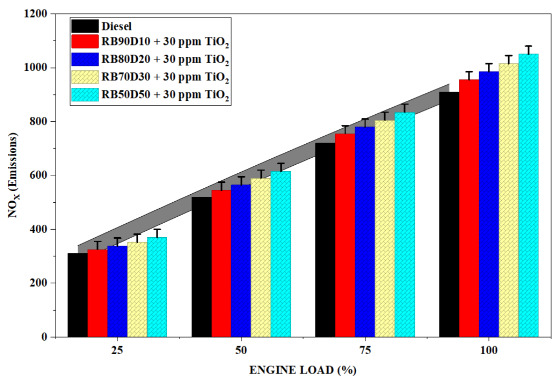

Figure 9. NO_x Emissions

6.5. Smoke opacity

Figure 10 shows the smoke opaqueness in the fuel/rice bran diesel-biodiesel blends with 30 ppm TiO_2 particles as the engine load increases. A key indicator of combustion deficiency in combustion-ignition vehicles is the amount of residual soot particles released from the exhaust, known as smoke visibility. The trend of improvement of exhaust opacity with performance is evident for all fuels analysed. Increased fuel injection required by higher combustion engine pressure leads to spatially rich air-fuel combinations and poor ventilation for compounds that contain carbon to oxidise completely [29]. All biodiesel-to-diesel blends have lower smoke opacity across the entire load range when compared to conventional diesel fuels. The highest smoke opacity of diesel is around 58%, much lower in the case of the nanoparticle mix. The lowest smoke opacity of the mixes assessed is RB50D50+30 ppm TiO_2 at 50 ppm. Diesel gets to 60 PPM. The end smoke opacity of the blend is 16% less than diesel. This is because rice bran fuel's basic oxygen content specifically promotes more complete breakdown of smoke precursors during burning, which is primarily responsible for the reduction in emitted smoke.

Additionally, by serving as a combustion catalyst, 30 ppm TiO_2 particles enhance fuel distribution and quicken oxidising processes in the flaming tanks. The stronger reactivity of the nanoparticles and the higher tendency of biofuel-containing droplets to undergo small explosions lead to improved air-fuel interactions and ignition. When combined, such findings reduce smoke opacity and prevent dirt from growing. Additionally, mixes with increasing biofuel percentage exhibit greater exhaust reductions since biofuel vehicles generate fewer volatile chemicals and contain higher levels of oxygen than diesel-powered engines. Among the tested options, RB50D50 + 30 ppm TiO_2 gives the greatest reduction in smoky opacity, indicating that it could be used as an environmentally beneficial fuel replacement for diesel-fueled processes [30].

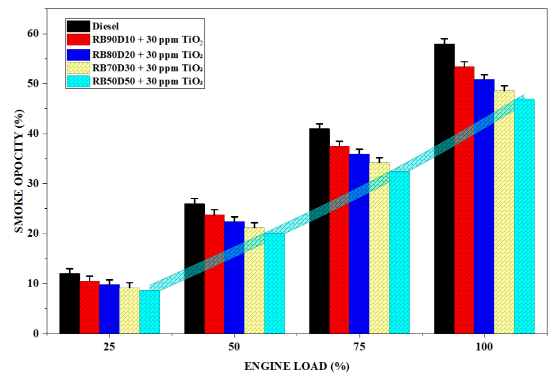

Figure 10. Smoke opacity

7. Conclusion

The present study analysed the fuel economy, efficiency, and pollutants of a typical piston combustion engine when rice bran biodiesel blends were supplemented with TiO_2 nanoparticles 30 ppm. The fuel blends that were assessed included RB90D10 + 30 ppm TiO_2, RB80D20 + 30 ppm TiO_2, RB70D30 + 30 ppm TiO_2, and RB50D50 + 30 ppm TiO_2. Normal diesel was used as the fuel. Results of the study reveal that significant enhancement in burning capacity is obtained with the addition of TiO_2 nanoparticles into normal rice bran biodiesel blends due to their catalytic effect, atomising conductance, and oxygen-neutralising property. RB50D50 + 30 ppm TiO_2 was a very good fuel for combustion, and RB70D30 + 30 ppm TiO_2 showed the greatest overall improvement in braking efficiency when compared to the other biodiesel blends. The maximum cylinder temperature was slightly higher for the TiO_2 nanomaterials than for the conventional biodiesel fuels due to faster reaction dynamics and higher thermal transfer efficiencies. This enhancement comes from the large radius and nitrogen-donating capacity of TiO_2 nanostructures, which bring about fuel-air interaction and accelerate oxidation processes in the combustion chambers. The nano combinations demonstrated a marked reduction in smoky transparency, residual hydrocarbon HC, and atmospheric carbon monoxide CO when compared to conventional diesel fuel. The decreases are mostly caused by improved oxidation processes made possible by extra oxygen atoms provided by rice-based bran fuel and TiO_2 nanoparticles. However, NO_x outputs increased slightly because of the high chamber heats and the high thermal conductivities of the mixtures used for the nano-boosting. In conclusion, the findings show that traditional rice bran biofuels supported by TiO_2 nanoparticles can be a viable alternative fuel for CI cars, with better fuel economy and lower emission rates without any vehicle modifications.

- The RB70D30 + 30 ppm TiO_2 mix has good brake thermal effectiveness, with a combined effectiveness of 37% at full load, whereas diesel achieves optimum brake thermal effectiveness at 34%. The effectiveness of the mix RB70D30 + 30 ppm TiO_2 is 8.8% better than diesel.
- At maximum throttle, the BSFC of the RB70D30 + 30 ppm TiO_2 mix is 0.22 kg/kWh, which is less than diesel's 0.25 kg/kWh. The mixture that has the lowest BSFC, 12% lower than diesel, is RB70D30 + 30 ppm TiO_2.
- The peak chamber pressure for each mix analysed was lowest for RB50D50 + 30 ppm TiO_2, at approximately 69 bar. The diesel pressure, however, is 65 bar. The RB50D50 + 30 ppm TiO_2 formulation is 6.2% more effective than diesel.
- The RB50D50 + 30 ppm TiO_2 blend has the highest peak heat release rate of 59 kJ/°CA of all the blends evaluated. Diesel achieves a heat release rate of 55 kJ/°CA. The blend RB50D50 + 30 ppm TiO_2 leads by 7.2% over diesel.
- The RB80D20 + 30 ppm TiO_2 blend generates 0.034% CO at full-throttle conditions, while diesel fuel achieves 0.05%. The RB80D20+ 30 ppm TiO_2 blend achieves the lowest emissions, 32 % lower than diesel.
- The RB50D50 + 30 ppm TiO_2 blend has approximately 12.6% CO_2 compared with diesel, whose value is significantly lower, at 10.5%. Accelerated ignition is made possible by the oxygenation nature of biofuels oils.
- The RB50D50 + 30 ppm TiO_2 blend is the second smallest with a 16.6% emitted level, followed by Diesel with an emitted level of 15.6%. • RB50D50 + 30 ppm TiO_2 and 22 ppm were the mixes with the lowest hydrocarbon footprints. Diesel, on the other hand, emits 42 ppm. The RB50D50 + 30 ppm TiO_2 blend is 47% cheaper than diesel.
- The nanoparticles produce standard mixtures; diesel produces around 910 ppm at max capacity. RB90D10 + 30 ppm TiO_2 is a product that generates 980 ppm of NOx emissions. It is 7.14% more than diesel.
- Of the blends tested, RB50D50 + 30 ppm TiO_2 at 50 ppm has the lowest smoky transparency. Diesel gets to 60 parts per million. The composite gets 16.6% less smoking density as compared to diesel.

Appendices

A/F	Air fuel ratio
ASTM	American Society for Testing and Materials
B10	10% Biodiesel + 90 % Diesel
BTE	Brake thermal efficiency
BMEP	Brake mean effective pressure
bTDC	Before top dead centre
BSFC	Brake specific fuel consumption
CeO_2	Cerium Oxide
DEE	Diethyl ether
RB90D10	90 % Ricebran oil + 10 % Diesel
RB80D20	80 % Ricebran oil + 20 % Diesel
RB70D30	70 % Ricebran oil + 30% Diesel
RB50D50	50% Ricebran oil + 50% Diesel
30 ppm	30 parts per million
CO	Carbon monoxide
CI	Compression Ignition
CA	Crank Angle
CO_2	Carbon dioxide
DEE	Diethyl ether
HC	Hydrocarbons
HHV	Higher heating value
HRR	Heat Release Rate
IMEP	Indicated mean effective pressure
NO_X	Nitrogen oxides
PM	Particulate matter
Ppm	parts per million
SEM	Scanning Electron Microscopy
SO	Sunflower oil
TiO_2	Titanium dioxide
TGA	Thermogravimetric Analysis
UHC	Unburnt hydrocarbons
XRD	X-ray Diffraction

Author contributions statement

Sunil Kumar – conceptualization and writing, original draft Review & editing. Methodology and analysis.

Data availability statement

The datasets used and or analyzed during the current study are available from the corresponding author on reasonable request.

Declaration of generative AI and AI-assisted technologies in the writing process

The authors would like to thank AI-powered writing tools, such as Grammarly, for their aid in enhancing the linguistic precision, correctness of grammatical structures, and the overall coherence of this article. All content, analysis and conclusions contained in this work are the author's own and are not in any way the work of AI. All content, analytical discussion and conclusions presented in this work are the sole work of the author and have not been generated using AI tools for any purpose other than to enhance the presentation and clarity of the text. The use of AI is aligned with the journal's standards of transparency and ethical guidelines in the authoring process.

References

[1] Alm-EldinBastawissi, H., Elkelawy, M., Elsamadony, M.O. and Ghazaly, M., 2025. Performance and Emissions Characteristics of Multi-Cylinder Direct Injection Diesel Engine

Fuelled with Diesel/Biodiesel and Toluene Additives. Journal of Engineering Research, 8(6), pp.29-37.DOI: 10.70259/engJER.2024.861809

[2] Köten, H. and Yılmaz, M., 2018. Advanced numerical and experimental studies on CI engine emissions. Journal of Thermal Engineering, 4(4), pp.2234-2247.https://doi.org/10.18186/journal-of-thermal-engineering.434044

[3] Selvam, C. and Devarajan, Y., 2025. Performance and emission analysis of sterculia foetida biodiesel enhanced with butanol: Combustion efficiency and emission mitigation. Results in Engineering, 25, p.104586. https://doi.org/10.1016/j.rineng.2025.104586

[4] Kumar, K.S., Muniamuthu, S., Khan, T.Y. and Razak, A., 2025. Performance evaluation of a diesel engine fuelled with waste plastic pyrolysis oil, 1-butanol, and CeO2 additives under varying injection pressures. Case Studies in Thermal Engineering, 72, p.106284. https://doi.org/10.1016/j.csite.2025.106284

[5] Devarajan, Y. and Selvam, C., 2024. Utilization of sterculia foetida oil as a sustainable feedstock for biodiesel production: optimization, performance, and emission analysis. ResultsinEngineering,24, p.103196. https://doi.org/10.1016/j.rineng.2024.103196

[6] PATEL, H.A. and PATEL, B.P., 2025. Investigation on performance and emission studies of variable compression ratio engine using neem oil biodiesel. Journal of Thermal Engineering, 11(6).DOI: 10.14744/thermal.0001049

[7] Yamini, K., Kishore, P.S. and Raju, V.D., 2025. Effect of diethyl ether and isobutanol as fuel additives on the diesel engine attributes fueled with subabul seed biodiesel. Journal of Thermal Engineering, 11(1), pp.215-225. https://doi.org/10.14744/thermal.0000914

[8] Enweremadu, C., Samuel, O. and Rutto, H., 2022. Experimental studies and theoretical modelling of diesel engine running on biodiesels from south African Sunflower and Canola Oils. Rigas Tehniskas Universitates Zinatniskie Raksti, 26(1), pp.630-647.

[9] Estevez, R., López-Tenllado, F.J., Aguado-Deblas, L., Bautista, F.M., Romero, A.A. and Luna, D., 2024. Evaluation of advanced biofuels in internal combustion engines: diesel/fusel oil/vegetable oil triple blends. Fuels, 5(4), pp.660-672. https://doi.org/10.3390/fuels5040036

[10] Ileri, E., Atmanli, A. and Yilmaz, N., 2016. Comparative analyses of n-butanol–rapeseed oil–diesel blend with biodiesel, diesel and biodiesel–diesel fuels in a turbocharged direct injection diesel engine. Journal of the Energy Institute, 89(4), pp.586-593..https://doi.org/10.1016/j.joei.2015.06.004

[11] Jayaraman, K., Anbuchezhiyan, G., Mubarak, N.M., Bandegharaei, A.H. and Abnisa, F., 2024. Exploring the combustion, emission and performance of n-Butanol with Deccan hemp oil methyl ester on dual fuel diesel engine. Scientific Reports, 14(1), p.28015. https://doi.org/10.1038/s41598-024-78966-3

[12] Khan, E., Ozaltin, K., Spagnuolo, D., Bernal-Ballen, A., Piskunov, M.V. and Di Martino, A., 2023. Biodiesel from rapeseed and sunflower oil: effect of the transesterification conditions and oxidation stability. Energies, 16(2), p.657. https://doi.org/10.3390/en16020657

[13] Khanna, S. and Gangele, A., 2025. Performance analysis of butanol-diesel blends in internal combustion engines as pathway to bioenergy integration toward sustainability goals. Next Energy, 8, p.100376. https://doi.org/10.1016/j.nxener.2025.100376

[14] Miao, R., Li, Y., Khanna, M., Clark, C., Burkholder, D. and Chen, L., 2026. Quantifying the land-use change due to soybean-based biodiesel in the United States. Applied economic perspectives and policy, 48(1), pp.20-47. https://doi.org/10.1002/aepp.70005

[15] Sakthimurugan, V. and Yuvarajan, D., 2025. A comprehensive assessment on recent advancements in spent fuel reprocessing and waste management: pioneering technologies for a sustainable nuclear future. Kerntechnik, 90(2), pp.125-138. https://doi.org/10.1515/kern-2024-0120

[16] Sunilkumar, K., Edayadulla, N., Raja, P. and Surakasi, R., 2023, July. The effect of emissions from DI-based sources causing hazardous health effects. In International Conference on Recent Advances in Mechanical Engineering Research and Development (pp. 1-13). Singapore: Springer Nature Singapore. https://doi.org/10.1007/978-981-97-1080-5_1

[17] Şimşek, D., Karabacak, Y., Çolak, N.Y. and Aksu, B., 2025. Optimization study of fuel blends in an SI engine running with gasoline/isopropanol/isoamyl alcohol blends. Bitlis Eren University Journal of Science and Technology, 15(1), pp.37-55. https://doi.org/10.17678/beuscitech.1500673

[18] Lin, L., Ying, D., Chaitep, S. and Vittayapadung, S., 2009. Biodiesel production from crude rice bran oil and properties as fuel. Applied energy, 86(5), pp.681-688.https://doi.org/10.1016/j.apenergy.2008.06.002

[19] El-Shafay, A.S., Abushammala, M.F., Elazab, M.A. and Gad, M.S., 2026. Comparative effects of Al2O3 and TiO2 nanoparticles with HHO enrichment on performance, emissions, and environmental assessment of diesel engine fuelled with waste tire–plastic co-pyrolysis oil. International Journal of Hydrogen Energy, 247, p.155802. https://doi.org/10.1016/j.ijhydene.2026.155802

[20] Sukjit, E., Klinkaew, N., Pumpuang, A., Batsungnoen, K., Thumthae, C., & Maneedaeng, A. (2025). Particulate matter characteristics and emissions of waste-and bio-derived fuels in diesel engine applications. Cleaner Engineering and Technology, 101056. https://doi.org/10.1016/j.clet.2025.101056

[21] Channapattana, S.V., Campli, S., Madhusudhan, A., Notla, S., Arkerimath, R. and Tripathi, M.K., 2023. Energy analysis of DI-CI engine with nickel oxide nanoparticle added azadirachta indica biofuel at different static injection timing based on exergy. Energy, 267, p.126622. https://doi.org/10.1016/j.energy.2023.126622

[22] Kumar, K.S., Munıamuthu, S. and Mohan, K.R., 2023. Measurement of temperature flow analysis by condition monitoring system for WTG gear box to evaluate the thermal performance associated with plant load factor. Journal of Thermal Engineering, 9(4), pp.979-987. https://doi.org/10.18186/thermal.1332437.

[23] Muniamuthu, S., Raju, N.L., Sathishkumar, S. and Kumar, K.S., 2016. Investigation on mechanical properties of Al 7075-Al2O3 metal matrix composite. International Journal of Mechanical Engineering and Technology, 7(6), pp.474-482.

[24] Yadav, N. K., & Maurya, R. K. (2025). Risk assessment of particle and gaseous emissions from diesel and methanol–diesel advanced dual-fuel engines. Biofuels, 16(7), 674-687.https://doi.org/10.1080/17597269.2025.2450165

[25] Zamparas, M., 2021. The role of resource recovery technologies in reducing the demand of fossil fuels and conventional fossil-based mineral fertilizers. In Low Carbon Energy Technologies in Sustainable Energy Systems (pp. 3-24). Academic Press. https://doi.org/10.1016/B978-0-12-822897-5.00001-8

[26] Devarajan, Y., Nagappan, B. and Subbiah, G., 2019. A comprehensive study on emission and performance characteristics of a diesel engine fueled with nanoparticle-blended biodiesel. Environmental Science and Pollution Research, 26(11), pp.10662-10672. https://doi.org/10.1007/s11356-019-04446-1

[27] Sunil Kumar, K., Babu, J.M., Venu, H. and Muthuraja, A., 2022. Waste plastic as a source of biofuel for stationary diesel engine: a critical review. International Journal of Ambient Energy, 43(1), pp.8577-8591.https://doi.org/10.1080/01430750.2022.2102074

[28] Vellaiyan, S., 2025. Development of sustainable diesel fuel blend using biodiesel, hydrous hydrazine and nanocatalysts for optimized performance and emission control. Case Studies in Thermal Engineering, 69, p.105966.https://doi.org/10.1016/j.csite.2025.105966

[29] Yuvarajan, D., Babu, M.D., BeemKumar, N. and Kishore, P.A., 2018. Experimental investigation on the influence of titanium dioxide nanofluid on emission pattern of biodiesel in a diesel engine. Atmospheric Pollution Research, 9(1), pp.47-52. https://doi.org/10.1016/j.apr.2017.06.003

[30] Atmanlı, A., Ileri, E. and Yüksel, B., 2014. Experimental investigation of engine performance and exhaust emissions of a diesel engine fueled with diesel–n-butanol–vegetable oil blends. Energy Conversion and Management, 81, pp.312-321. https://doi.org/10.1016/j.enconman.2014.02.049